Work Statement

In 2018, I joined Peking University as a tenure-track assistant professor. My research concentrates on the experimental study of varies quantum phases in two-dimensional electron/hole systems (2DES/2DHS). We have significantly improved or successfully developed several measurement techniques, including capacitance, Surface Acoustic Waves (SAW), magneto-optical-Kerr-Effect (MOKE), etc., and discovered many interesting phenomena using these new probing tools.

Section I: Lab

Our laboratory locates at the E-wing of the physics building, having one ground floor room E105 and E206 right above it. We have installed two top-loading Oxford Triton 400 dilution refrigerators. We carefully designed cryo-temperature low-pass filter boxes for our DC wires. The filters can attenuate signals from ~100 MHz up to 20 GHz (>50 dB). We have installed 6 low impedance semi-rigid coaxial cables in each fridge. The mixing chamber temperatures of both systems remain <10 mK after the modifications. Besides the two dilution fridges, we are currently working with Lin Xi to build a multi-purpose 4-K fridge and integrate multiple unique measurement capabilities.

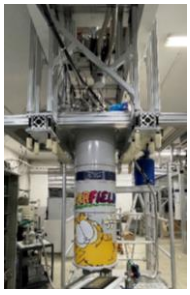

Fig. 1 We have two top-loading Triton 400 systems. The rear system has a 14 T magnet with cancellation coil. The front system has a 91 mm bore size 12 T magnet. The loading and measurement are performed in the up-floor room. We designed a special mounting structure for the front system. Two steel beams are anchored at the building framework, to which the dilution fridge is hanged with 16 20-mm steel rods (inside the vertical aluminum profiles). The fridge has a clear surrounding and the structure and the load bearing is over 3,000 kg.

Our 14 T magnet has a cancellation coil so that the magnetic field at the mixing chamber plate is significantly suppressed. We have designed, manufactured and tested all-plastic low-eddy-current sample puck. This puck maximizes the sample space and minimizes the eddy current by removing all unnecessary metal parts. As shown in Fig. 2, we are able to seep the magnetic field at 0.25 T/min while keeping the mixing chamber temperature at about 10 mK.

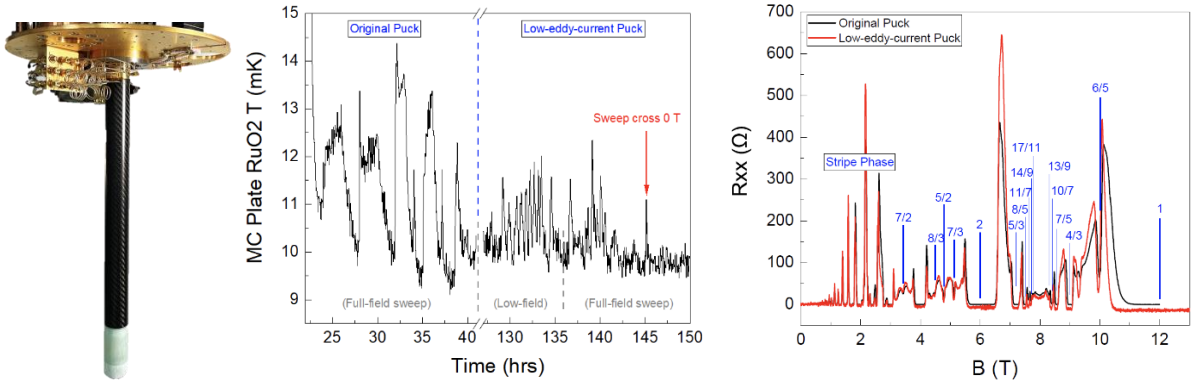

Fig. 2 Our low-eddy current puck for maximizing the sample space and the sweep rate. Left: the image of our puck. Middle: comparing the eddy current heating of our design and Oxford standard puck when

sweeping magnetic field at 0.25 T/min rate. The mixing chamber temperature remains at about 10 mK when using our design, while it increases by a few mK using Oxford standard puck. The temperature spikes appear near zero magnetic field, possibly caused by the ferromagnetism of the thermometer. Right: the magneto-resistance of a high mobility 2DES sample measured using Oxford (black) and our puck (red).

Our 12 T magnet has a 91 mm bore size, enabling the installation of multi-function sample stages. We installed a 3-axis piezo step motor and optical fiber. We are able to perform high resolution optical measurements at mK temperature inside this system, see Fig. 3.

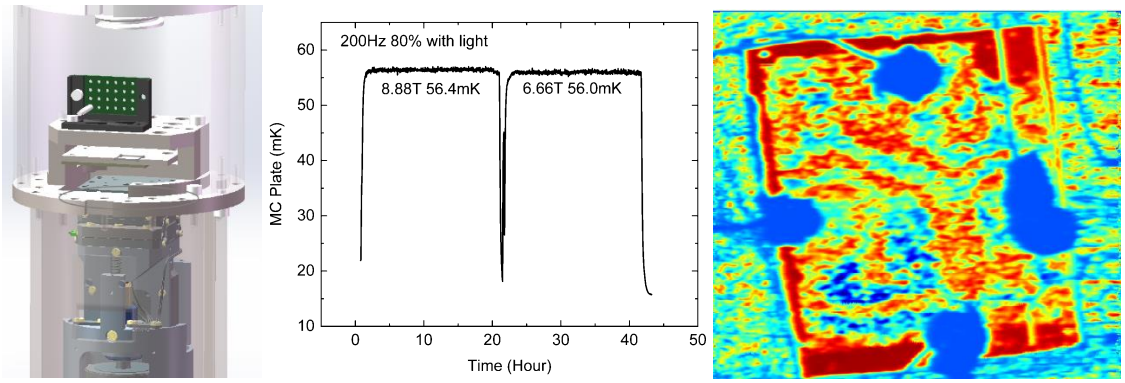

Fig. 3 The sample stage with 3-axis scanner. Left: the 3-axis piezo step scanner is installed on the still shield, the sample is installed facing down on the plate and thermally anchored to the mixing chamber cold finger. Middle: the mixing chamber temperature is stable at about 56 mK when the scanner moves at about 10 μm/s. Right: a typical MOKE image of a 1.5 x 1.8 mm size InAs 2DES sample taken at 8.8 T.

See below the timeline of our lab construction and technique development:

Section II: Our Special Measurement Techniques

Developments in condensed matter physics usually involve joint progresses in theory, material growth and measurement techniques. Our group studies quantum phenomena using advanced, non-regular measurement techniques. For all these techniques, we optimize their resolution while keeping the excitation as low as possible. After joining ICQM, we have significantly improved or successfully developed several measurement techniques, including:

- Inventing a new approach to precisely measure sub-fF capacitance at mK-temperature.
- Improving the experiments utilizing SAW. We can use sub-pW acoustic power to probe quantum phases while achieving resolution better than previous works.
- Integrating μrad-resolution MOKE measurement with in-situ scan-imaging capability at mK-temperature.
- Inventing a contactless dilatometer using optical interferometer. We can resolve pm-level thermal expansion, comparable with the state-of-the-art capacitance dilatometers.

Despite the vast differences between the above techniques at the first glance, they actually share common features and are complementary to each other.

- We develop a radio-frequency (RF) lock-in amplifier that can analyze signals as small as -160 dBm whose frequency ranges from <10 MHz up to 4 GHz. Therefore, we are able to perform capacitance, SAW and MOKE measurements with extraordinarily high resolution.
- We developed a sample stage with optical fiber whose thermal expansion is carefully taken care so that light can be efficiently coupled from room temperature to mK temperature. This capability not only enables the MOKE measurement, but also the interferometer-based dilatometry measurement.
- We can use the optical fiber interferometer to measure thickness change of the samples, which is an important tool when experiments involve straining the samples.
- Our optical setup can reveal the propagation of surface acoustic wave, helping us to improve the SAW device.

The functioning principle of the RF lock-in amplifier can be described as:

a. Three signal-frequency signals, V_{in}, V_{LO} and V_{ref}, are generated from the same clock f_{CLK}. Their frequencies are f_{in}, f_{LO} and f_d, respectively, and $f_d = |f_{in} - f_{LO}|$.
b. V_{in} is sent to the device which attenuates its amplitude and introduces a phase delay θ.
c. The output signal V_{out} will be amplified and then multiplied with V_{LO} at the mixer. We then use a filter to extract the differential frequency component V_d.
d. The information of V_{out}, *i.e.* its amplitude and phase, is transferred to V_d. $|V_d|$ is proportional to $|V_{out}|$, and θ_d (the phase difference between V_d and V_{ref}) differs from θ by a constant.
e. We measure $|Vd|$ and θ_d using a digital audio-frequency lock-in unit.

A: High precision capacitance measurement

We develop a new method for high precision, low excitation capacitance measurement from 10 mK to room temperature. We install a passive bridge which is mounted on the sample holder inside the cryostat, and in-situ tune its balance using a high-electron-mobility-transistor (HEMT) as a voltage-controlled-variable-resistor. We increase the excitation frequency to >10 MHz and develop a high sensitivity RF lock-in technique to analyze the output signal.

The power dissipation of setup is only ~ 10 nW so that this setup can be used at temperatures as low as 10 mK. In addition, we measure the resistance in-situ so that we can perform continuous measurement when temperature changes from 10 mK to 300 K. We are able to measure the absolute capacitance value by balancing the bridge and reach < 0.1 pF accuracy after calibration. With about 1 mVrms excitation voltage, we can resolve 240 ppm variation of a 500 fF capacitor (0.1 fF), see Fig. 4. We introduce an impedance match network so that the measurement frequency ranges from 7 to ~100 MHz.

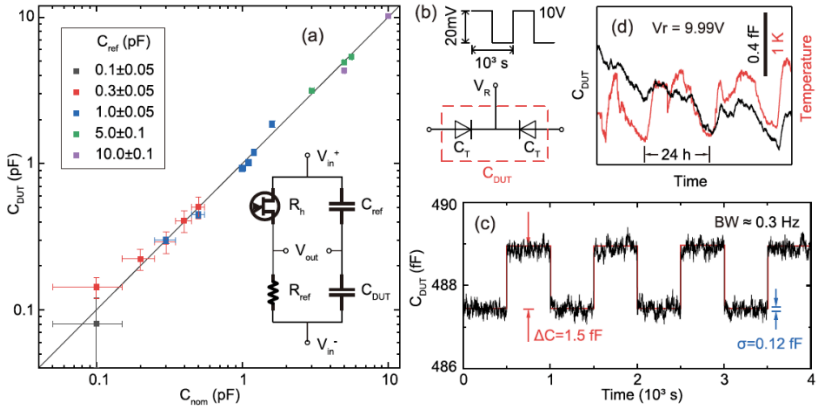

FIG. 4. Calibration of our capacitance setup in fridge at room temperature using commercial capacitances. (a) C_{DUT} is the measured capacitor values by balancing the bridge. C_{nom} is their nominal value given by manufacturers. The error bar is deduced from their tolerance. Data points with different colors represent different C_{ref}, and the black line is the ideal $C_{DUT} = C_{nom}$. (b) Measuring two back-to-back connected tunable capacitance diodes. The reverse voltage V_R tunes the value of each diode capacitance C_T. V_R is a 1000-second-period, square wave with high/low voltages equal 10/9.98 V. (c) Measured C_{DUT}. $C_{DUT} \approx 487.5$ fF for $V_R = 10$ V and increases by 1.5 fF when V_R decreases by 20 mV. The standard deviation is as low as 0.1 fF at 0.3 Hz measurement bandwidth. (d) Long period monitoring of C_{DUT} with V_R fixed at 9.99 V (black), as well as the room temperature (red).

B: Surface Acoustic Waves (SAW)

SAW is also a useful current-free technique to investigate the transport property of 2DES. The traveling electric field accompanying the SAW interacts with the charge carriers, which in turn affects the sound velocity and attenuation. Qualitatively, this interaction strength is related to the compressibility of 2DES. The SAW velocity is large when the 2DES forms incompressible quantum Hall liquid and decreases if the 2DES is compressible.

We improved the heterodyne scheme lock-in amplifier which now functions from 50MHz to 2 GHz and has ultra-high phase sensitivity. We use fractional phase locked-loop (PLL) to generate two signals V_{in} and V_{LO}, whose frequencies are locked to the reference clock frequency f_{CLK} through $f_{in}/f_{CLK} = N/M$ and $f_{LO}/f_{CLK} = (N+K)/M$, respectively; N, M and K are integer values. We properly choose the internal Direct Digital Synthesis module to generate a third signal V_{REF} at $(K/M)f_{CLK}$ and use it as the reference signal. The feedback loop within the two PLLs suppresses their phase jittering. The measured phase noise spectral density is proportional to $1/f^{0.5}$ and equals about 0.2 mrad/Hz$^{0.5}$ at 1 Hz.

C: High performance MOKE measurement at mK

We install optical-fiber into the dilution refrigerator to explore the possibility of studying 2DES using optics. We start with MOKE measurements using an all-fiber zero-loop Sagnac interferometer following previous works by Kapitulnik group (Jing Xia, et al. APL 2006). We use the heterodyne scheme to improve its low-power performance. We are able to measure MOKE at sub-10 mK, using 5 μW input optical power and the noise spectrum density is 40 μrad/Hz$^{0.5}$ (< 5 μrad with 100s averaging time). We have installed a three-axis piezo scanner cooperating with a focusing gradient-index lens, which allows spatial mapping with resolution of 15 μm. We can successfully take MOKE images at <100 mK temperatures.

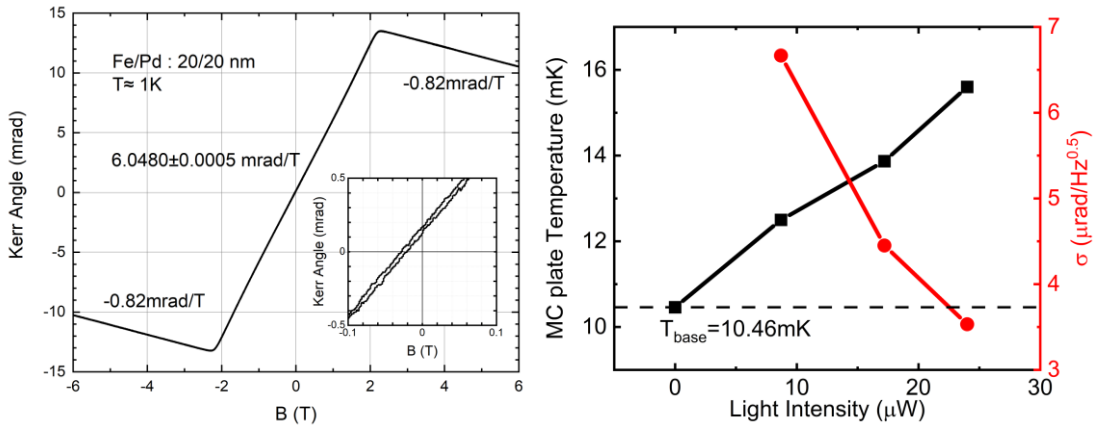

Fig. 5 MOKE system calibration. Left: Measured MOKE signal of a 20-nm Fe layer. The layer is in-plane ferromagnetism, resulting in a linear MOKE signal at low field. The MOKE signal reaches maximum at about 2 T perpendicular field, consistent with the fact that Fe layer becomes out-of-plane polarized. The decrease of MOKE at high field is also consistent with the diamagnetism of free electrons in metal films. Right: The noise density and mixing chamber temperature at different input light power. We are able to achieve < 10 μrad/Hz$^{0.5}$ noise at < 20 mK temperature with 10 μW input optical power.

D: High precision AC dilatometry

We developed a high-stability optical fiber interferometer to test the optical coupling, to study the propagation of SAW, to calibrate the deformation of sample under strain, etc. Based on this setup, we developed an AC dilatometer which measures the sample thickness variation contactlessly. Our setup is "truly" differential where the applied temperature oscillation induces an oscillation in sample thickness. We then deduce the thermal expansion coefficient α using lock-in technique. We achieve sensitivity comparable to the best reported capacitive dilatometry, i.e. pm-resolution in thickness oscillation amplitude when using mK-amplitude temperature oscillation.

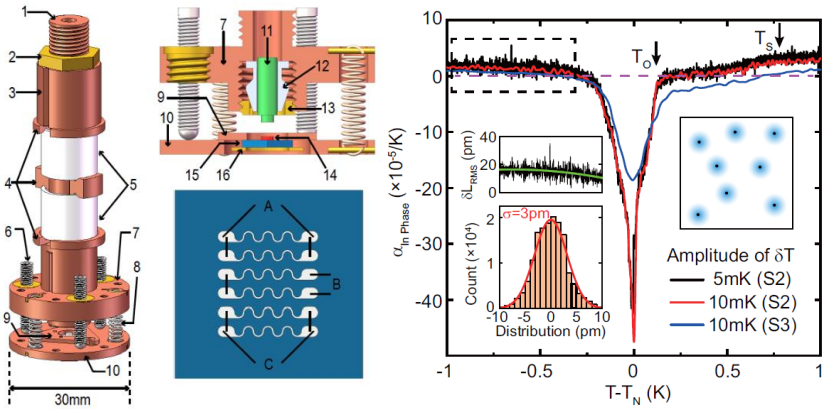

Fig. 6 Left: The cold finger of our dilatometer sample stage. The probing and reference arms of the fiber Michelson interferometer are winded around the PZT rings (white cylinder labeled 5) by which we can tune their length using the modulation and feedback voltages. The grin lens (11) is used to focus light onto the sample (14). We evaporate meadow Pt wires on the sapphire sample holder (blue cartoon) and use them as thermometer, AC and DC heaters. Right: Measured thermal expansion coefficient α using mK-level

temperature oscillation. The x-axis is T-T_N for better comparison. The left inset shows the measured thickness oscillation amplitude in the range marked by the two vertical bars using 50 mHz resolution bandwidth. We deduce 3 pm resolution from the histogram of noise after subtracting the fitted green curve.

Section III: Physics Discoveries

Conventional transport measurement of quantum system usually studies their ground state properties, such as compressible/incompressible, conducting/insulating, polarized/unpolarized. In our studies, we focus on studying the dynamical response of different quantum phase, i.e. the morphing of quantum phases when an external field is applied. Our capability of integrating different high-sensitive techniques enables the detection of small variation of a correlated system. This is a rather new topic in experimental condensed matter physics, and many of our techniques are sufficiently innovative, so that we are able to discover phenomena that have never been expected. Therefore, *it is our obligatory duty to patiently exclude all sorts of experimental artifacts, reproduce the results, and corroborate the data consistency.* We are convinced after I had thorough discussions with talent and experienced community fellows at the EP2DS and QP2DM workshop in the summer of 2023. We are now busy summarizing the results and expect to finish these manuscripts in the coming few months. In this section, we will briefly list some of our new descoveries.

A: Probing Wigner crystal using capacitance measurement

Capacitance measurement is a very practical technique to characterize the electronic properties of 2DES. The total capacitance between the gate and the 2DES has two components: one is the geometric capacitance C_G from the voltage drop in the insulating spacer between gates and the electron layer, the other one is the quantum capacitance $C_Q = e^2\,\mathrm{d}n/\mathrm{d}\mu$. The macroscopic quantum transitions in a condensed matter system usually changes its compressibility, *e.g.* density of state $\mathrm{d}n/\mathrm{d}\mu$ at the Fermi energy of a Fermi sea, which can be directly probed by high resolution capacitance measurement. Unfortunately, this is not a sufficient description of capacitance in ultra-high mobility 2DES. Firstly, the occupation of second subband is usually seen as increasing electron density which also induces variation of charge distribution, leading to a changing of the geometric capacitance. Secondly, the sheet conductivity of 2DES may also affect the movement of electrons so that the effective charging area is no longer the same the gate area.

In the first demonstration of our technique, we carefully study a sample consists a 650-Å-wide quantum well resides 1665 Å below the surface. In this sample, an additional 2DES forms at the interface between the substrate-side spacer-layer and the GaAs buffer layer, which we can use as a reference. We observe four capacitance plateaus corresponding to four different scenarios of the charge distribution. The width and height of these plateaus can be used as precise probe of the electron charge distribution.

In a continuous study, we find that the capacitance of ultra-high mobility 2DES samples decreases dramatically from its $B = 0$ value by orders of magnitude as B^{-3}, because their longitudinal conductance decreases as B^{-2}. We find that the device capacitance C strongly entangles with the 2D conductance as $\mathrm{C} \propto \mathrm{G}^{2/3}$. In short, a zero capacitance may not evident the vanishing quantum capacitance of an incompressible state, but is possible a mere adjunct to the vanishing conductance of an insulator.

We then investigate the capacitive response of electrons at the extreme quantum limit ($\nu \ll 1$) and near the integer fillings ($\nu = N$, $N = 1, 2, 3, \ldots$), where the Wigner crystal is expected to be the ground state. It shows a very large capacitance while the conductance vanishes. This large capacitive response arises from the polarization current of Wigner crystal. We can then deduce the correlation length, dielectric constant and elastic modulus, etc. quantitatively by modeling the dynamic response of the Wigner crystal.

In another work, we examine the 2DES confined in wide quantum wells whose subband separation is comparable with the Zeeman energy. Our results indicate that two N = 0 Landau levels from different subbands and with opposite spins are pinned in energy when they cross each other and electrons can freely transfer between them in a large range of B. This is because that the electrons' redistribution between the two crossing Landau levels competes with the 2DES's Hartree potential which prevents any abrupt charge transfer by introducing renormalization of subband separation. When the disorder is strong, we observe clear hysteresis in the capacitance corresponding to instability of the electron distribution in the two crossing levels. When the intra-layer interaction dominates, multiple minima appear when a Landau level is 1/3 or 2/3 filled and fractional quantum Hall effect can be stabilized. Our observations shed light on the complex internal structure of 2DES when multiple subbands present.

B: Probing the quantum Hall effect with SAW

SAW is a useful technique to investigate the transport property of 2DES. The traveling electric field accompanying the SAW interacts with the 2DES, which in turn affects the sound velocity and attenuation. Qualitatively, this interaction is related to the compressibility of 2DES. The SAW velocity is large when the 2DES forms incompressible quantum Hall liquid and decreases if the 2DES is compressible.

With the help of our newly developed RF lock-in technique, we probe the 2DES using a pW-level SAW with an extremely high phase sensitivity. The typical input RF power in our study is 1 pW to 1 nW (-90 to -61 dBmW), and only a tenth of which turns into SAW. The SAW induced potential on the 2DES is less than 20 μeV, leading to about ~10^5 cm^{-2} induced charge fluctuation.

In our first work, we discovered that the ~ 100 nA current flowing through the ~1 mm size sample causes ~0.1 ppm (parts per million, 10^{-6}) increase of the SAW velocity at very low temperatures T < 250 mK. Such a current-induced velocity increase illustrates that a close and careful examination on the current flowing mechanism is essential and imperative.

On the other hand, the propagating SAW will drive and transfers momentum and energy to charged particles and cause a finite drag current. We carefully optimize the setup, such as using coaxial wires to reduce crosstalk, building compact transimpedance amplifiers for low input impedance and well-isolated current loop, etc. Besides the drag current, we notice that the 2DES conductance can be tuned by SAW at the flanks of quantum Hall plateaus. Similar to previous studies, the measured drag current is finite when 2DES is compressible and exhibits minima at exact integer fillings, if the SAW is strong. When reducing the SAW power, the drag current at the compressible state decreases linearly.

Counterintuitively, we find sharp current peaks near integer fillings within the quantum Hall plateaus at very low SAW amplitude. The drag current is zero at exact integer, and has opposite polarity on the two sides of exact integer filling. We speculate that the this abnormally large current comes from the dissipation-less transport of the incompressible quantum Hall liquid. The reversing of current direction is likely caused by reversed quasiparticle charges on the two sides of exact fillings. This current peak within the plateau can be seen from the inner contact to the outer contact of a Corbino geometry sample. Thus, SAW can drive current through the incompressible bulk.

C: Quantum oscillation in MOKE

When a linearly polarized light incident onto a sample located in magnetic field, the polarization axis of reflected light rotates due to the magneto-optical Kerr effect (MOKE). MOKE measurement can reveal the interaction between photon and electron spin and angular momentum through spin orbital coupling.

Its direct, non-contacting and high sensitivity properties are suitable for studying phase transition involving time reversal symmetry breaking, like ferromagnetic transition.

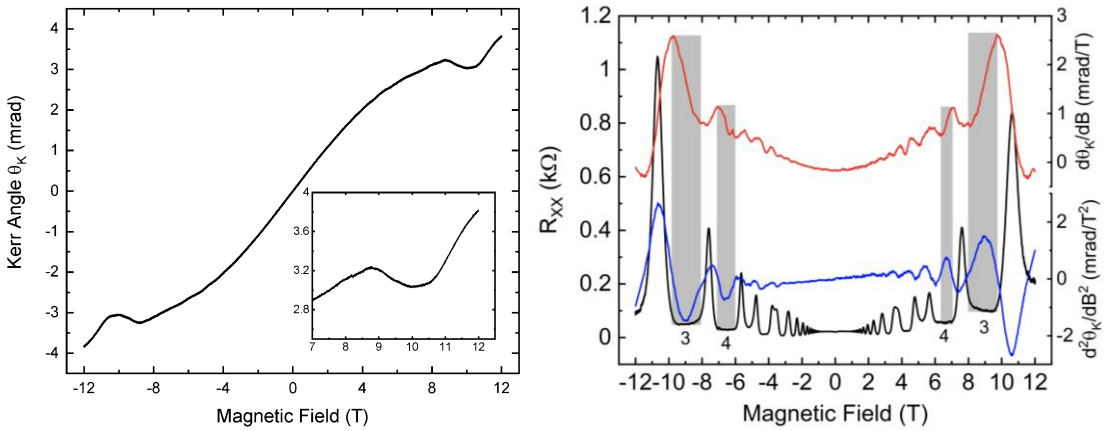

Fig.7 Kerr effects and transport measurement of 2DESs in InAs/GaSb quantum well. Left: Kerr angle θ_K is nearly proportional to the magnetic field. Inset is the zoom-in diagram near $\nu = 3$ (9 T). Right: Derivative of θ_K shows oscillations matching with quantum hall plateaus (gray area).

We investigate 2DES in high quality InAs/GaSb quantum well. We find many unexpected features which calls for further in-depth investigation and modelling. The MOKE signal has a mrad-order component that is proportional to magnetic field, possibly origins from the large Hall conductivity σ_{xy} of the 2DES and enhanced by the surface plasmonic mode. In doped samples, MOKE signal has a large fluctuating component across the sample, possibly due to the doping layer as well as the residual strain in the substrate. Thanks to the high resolution of our setup, we can observe clear oscillation in our Kerr signal, which matches the R_{xx} oscillation in transport perfectly.

D: AC Dilatometry and phase propagation speed

Using our AC dilatometry, we examine the phase transitions in BaFe2As2. It is the parent compound of the "122" Fe-based superconductors, and is generally believed to have a two-step paramagnetic (PM) to antiferromagnetic (AFM) phase transition when temperature reduces, i.e. a second-order structural transition at $T_S = 134.5$ K followed by a first-order magnetic transition at $T_N = 133.75$ K. Our results reveal a hysteresis at the transition temperature whose width in temperature is proportional to the sample thickness as well as the frequency and amplitude of the AC temperature oscillation. We can describe this dynamic process with a simple model and our systematical study reveals a propagation speed of the phase boundary to be $v = 188$ μm/s. The fact that this speed is significantly smaller than the acoustic velocity, sheds light on the complex nature of domain boundary dynamics. This work demonstrates that dilatometry with extraordinarily high resolution is a powerful probe of correlation effects in quantum materials.

Section IV: Ongoing and future projects

We have already mastered the above techniques and demonstrated their power in studying interesting physics. We are now working on several projects to understand our current observations as well as exploring new unexpected phenomena. We introduce some example ongoing projects:

We are now continuing the study of the Wigner crystal. In this project, we will study the elastic modulus and pinning potential of Wigner crystals in 2DES with controllable disorder and compare these parameters with the resonance frequency measured using microwave coplanar waveguide by Lloyd Engle at NHMFL. These samples will be grown by Loren Pfeiffer and Mansour Shayegan at Princeton university. We are also working on a project to study the Wigner crystal of electron-on-Helium system with Cheng Zhigang group. Our capacitance measurement is usually more sensitive than the transport measurement. We are now working with many collaborators to study different 2D materials, such as twist graphene, MnPS, MoS2, etc.

Thanks to the low SAW power used in our study and the high resolution, we have observed very interesting phenomenon, such as current induced velocity shift, large drag current, etc. We are now exploring the relation between different observations, and working with collaborators to understand the physics. These studies will significantly enhance our understanding of transport mechanism of incompressible quantum Hall liquid. Our preliminary data has demonstrated the possibility of using SAW to observe quantum oscillations in graphene, NbSe, etc. We are now optimizing our technique so that we can use this method to study 2D materials, or interface superconductivities, etc.

MOKE setup is a powerful tool in studying magnetic materials. In the future, we are planning to expand this setup by including pump/probe method, using different optical wavelength, etc.

We have demonstrated the power of our optical-interferometer-based dilatometer. We are planning to work on integrating this setup into magnetic field and lower temperature, so that it can probe magnetic transitions, ferroelectricity, as well as electronic transitions of surface/interface state, etc.

Section V: Collaborations

Our capability of performing high quality measurements with non-standard techniques is valuable complementary to the community and has received great interests from many colleagues. We have established collaborations with many research groups inside and outside Peking university.

- We are collaborating with Mansour Shayegan group at Princeton university and Lloyd Engle group at NHMFL, continuing our study of Wigner crystal.
- We have collaboration with Chen Jianhao and Lu Xiaobo groups on the quantum capacitance study of different 2D-material systems, such as graphene, MPS, etc.
- We are now working with Lin Xi group to study high mobility 2DES using SAW. We are also working together studying the quantum phase transitions of 2DHS under hydrostatic pressure or uniaxial strain.
- We have collaboration with Cheng Zhigang group at IOP studying the electron-on-Helium system.
- We have collaboration with Jia Shuang and Wang Jian groups with MOKE measurement. We observed anomalous features in Kerr angle near the Neel temperature of CoSnS and TeMnSn.
- We are currently working with Du Ruirui group to study geometric resonance and commensurability of anti-dot 2DES using MOKE measurement.
- We have collaborated with He Qinglin group, studying ferromagnetic phase transitions in magnetic thin films with MOKE.
- We are working with Li Yuan group to study materials using dilatometers, SAW, etc. to detect the broken symmetries in these materials, which will be further investigated by Neutron scattering.
- We are now collaborating with Liang Tian at Tsinghua University on a project to develop a measurement setup to study the magneto-electric effect in topological materials.